InGaAs/InP and Ge-on-Si SPADs for SWIR applications

Alberto Tosi, Fabio Signorelli, Fabio Telesca, Simone Riccardo, Enrico Conca
Dipartimento di Elettronica, Informazione e Bioingegneria, Politecnico di Milano
Piazza Leonardo da Vinci 32, 20133 Milano, Italy
E-mail: alberto.tosi@polimi.it

Abstract Many applications, like eye-safe LiDAR and quantum communications, require single-photon detectors for the SWIR range with high detection efficiency up to 1550 nm. Here, SPAD detectors fabricated in either InGaAs/InP or Ge-on-Si technologies will be reviewed, showing that the more mature InGaAs/InP SPADs have better performance, but Ge-on-Si ones might be considered in the future as cost-effective alternatives.

Keywords: Single Photon Avalanche Diode (SPAD), InGaAs, InP, germanium, photon counting, SWIR, Light Detection and Ranging (LiDAR), quantum imaging, quantum communications

1. Introduction

InGaAs/InP Single-Photon Avalanche Diodes (SPADs) [1] are among the preferred solutions for detecting single photons in the short-wave near infrared (SWIR) range in applications like quantum communication [2], quantum optics experiments [3], eye-safe light detection and ranging (LIDAR) [5], and near infrared spectroscopy (NIRS) [6]. As opposed to other superconducting detectors operating at cryogenic temperatures, InGaAs/InP SPADs are integrated in compact, reliable and easy-to-used systems, but they have limited maximum count rate (due to afterpulsing) and they cannot be integrated with standard CMOS circuits for developing wide photon counting imagers. As an alternative, Ge-on-Si SPADs benefit from the good absorption properties of germanium in the SWIR range and can be integrated onto a CMOS-compatible silicon substrate, thus achieving cost-effective solutions and being suitable for wider deployment in many different applications. Additionally, Ge-on-Si SPADs feature low afterpulsing, so that higher photon count rate can be achieved. However, state-of-the-art Ge-on-Si SPADs show a high dark count rate (DCR) also at low temperatures, because of the dislocations generated by conventional Ge/Si epitaxy [7].

2. InGaAs/InP SPADs

InGaAs/InP SPADs are based on the separate absorption, grading, charge and multiplication (SAGCM) heterostructure, as shown in Figure 1 [1]. A single SWIR photon can be absorbed in the low energy gap (E_g = 0.75 eV at 300 K) $In_{0.53}Ga_{0.47}As$ layer and the photogenerated hole is drifted towards the high electric field multiplication region made in InP (E_g = 1.35 eV at 300 K), where a self-sustaining avalanche can be triggered, thus generating a macroscopic current pulse that is easily read by an external circuitry.

In our frontside illuminated planar detector, a double zinc diffusion defines the active area of the detector: the electric field is high under the deep diffusion, while it is low under the shallow diffusion. Depending on the detector sizing, a floating guard ring can be included. A charge layer is present between the absorption and the multiplication regions for properly shaping the electric field, while quaternary InGaAsP grading layers are needed for reducing the valence band discontinuity [8][9].

The photon detection efficiency of SPAD detectors is calculated from two contributions: i) the absorption probability of a photon in the InGaAs layer, P_{abs}; ii) the avalanche triggering probability that a photo-generated hole triggers a self-sustaining avalanche, P_{trig}. Therefore, the photon detection efficiency is PDE = $P_{abs} \cdot P_{trig}$. Figure 2 shows the PDE dependence on the photon wavelength: PDE can be as high 40% around 1 µm, while it is more than 25% at 1550 nm. Starting from optical and electrical simulations, and selecting the most suitable models for

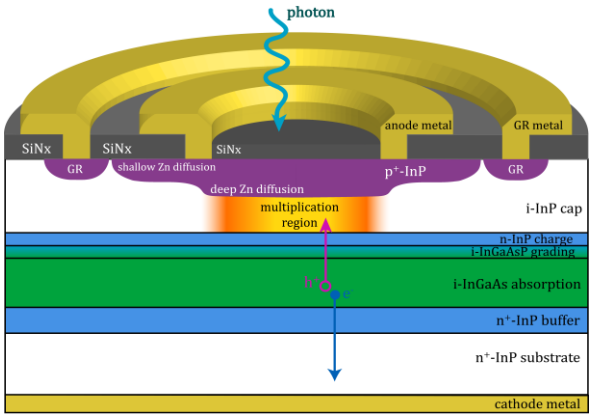

Figure 1 - Cross-section of the front-illuminated InGaAs/InP SPADs. Single photons enter the front window and can be detected in the InGaAs absorption layer. The photogenerated hole is drifted towards the high-field InP multiplication region, where it can trigger a self-sustaining avalanche multiplication, thus generating a strong current pulse in response to a single photon.

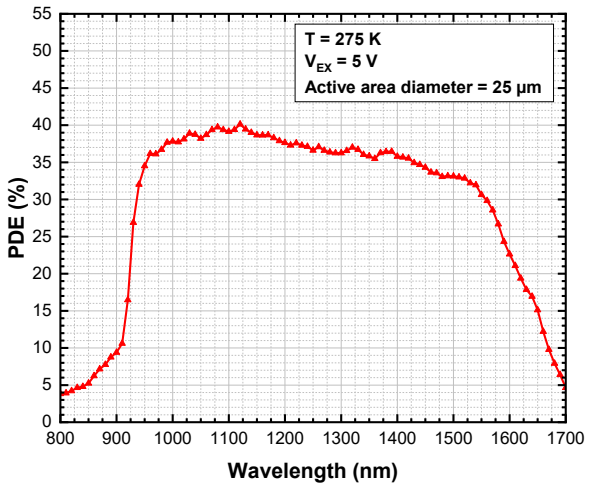

Figure 2 – Photon detection efficiency (PDE) of InGaAs/InP SPADs as a function of wavelength. PDE do not change significantly even down to 230 K.

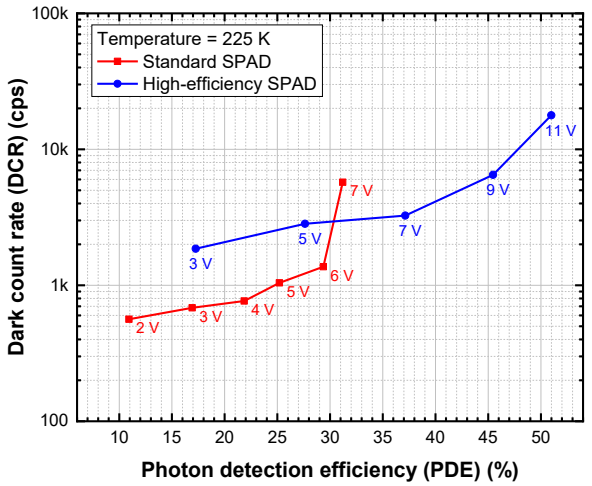

Figure 3 – DCR as a function of PDE for standard and high-efficiency detectors (both detectors have 25 µm active area diameter), measured focusing a 1550 nm laser spot inside the active area. The excess bias voltage V_{EX} for each measurement point is reported nearby each data point.

the refractive indexes, ionization coefficients and minority carrier lifetime (including their temperature and doping dependences), we developed a PDE model that guarantees good agreement between measurements and simulations [10].

In order to enhance PDE, in high-efficiency InGaAs/InP SPADs we increased the thickness of the absorption layer to ~ 2 µm, so that about 50% more photons are absorbed compared to the standard device. However, the thicker InGaAs layer brings also disadvantages: i) higher dark count rate; ii) reduced active area uniformity; iii) possible premature edge breakdown. In order to solve such issues, we tailored its internal structure (shape and depth of the double zinc diffusions) and we also added a guard ring (GR) with its dedicated bonding pad in order to better control the electric field at the device edge.

Figure 3 shows the measured PDE at 1550 nm and the corresponding dark count rate (DCR) value for both standard and high-efficiency InGaAs/InP SPADs. In all the measurements here reported, SPADs were operated in gated mode, where the detector is ON (by increasing its bias voltage beyond the breakdown by an amount call excess bias voltage

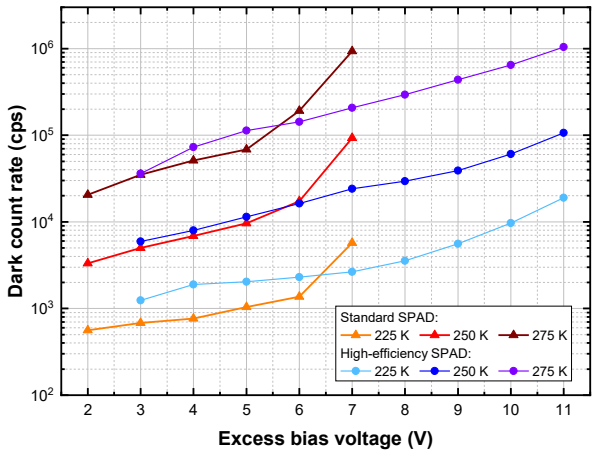

Figure 4 – Dark count rate of standard and high-efficiency SPADs (both detectors have 25 µm active area diameter) as a function of the excess bias voltage at different operating temperatures.

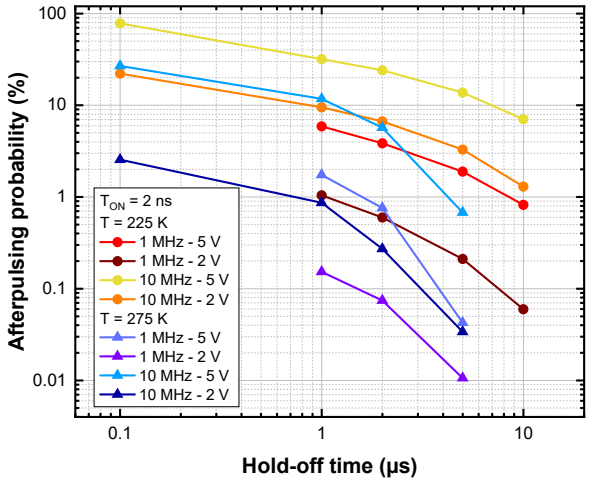

Figure 5 – Afterpulsing probability of a standard 25 µm InGaAs/InP SPAD as a function of hold-off time, measured with time-correlated carrier counting technique, at two temperatures. Measurements are taken at different excess bias voltages V_{EX} and gating frequencies f_{GATE}. Gate-ON time is T_{ON} = 20 ns.

V_{EX}) for a well-defined time interval T_{ON}, whose repetition frequency is the gate frequency f_{GATE}. The standard SPAD reaches a PDE just below 30% with a DCR of ~1 kcps, while it features a PDE higher than 10% with a DCR as low as 600 cps. The high-efficiency SPAD shows a PDE above 50% with a DCR below 20 kcps. At V_{EX} = 7 V, this device shows 37% PDE with a low DCR ~ 3 kcps. Comparing the two devices, the standard SPAD is the best choice for PDE up to 30%, while the high-efficiency SPAD is better if a higher efficiency is needed, as it shows lower DCR.

Figure 4 shows the DCR dependence on both excess bias voltage and temperature: high-efficiency SPAD has high DCR (almost twice) compared to standard one, due to thicker (almost twice) absorption layer.

Afterpulsing is one of the main drawbacks of InGaAs/InP SPAD and it is given by avalanche carriers getting trapped and released from deep levels. Release times can be quite long, thus requiring long hold-off times after each avalanche for emptying the traps when the detector is off.

We characterized the afterpulsing probability with the detector operated by an application-specific integrated circuit that we developed for InGaAs/InP SPADs. It is fabricated in 0.16 µm BCD (Bipolar-CMOS-DMOS) technology and it is capable of fast-gating SPADs at a maximum excess bias of 5 V and a gate frequency of up to 100 MHz. Avalanche quenching is completed in < 2 ns, thus keeping the avalanche charge at a low level. The SPAD and its front-end circuit are hosted onto a small carrier with a thermistor for temperature sensing, and placed on top of a 4-stage thermo-electric cooler within a bespoke vacuum chamber.

Figure 5 shows the afterpulsing probability calculated with time-correlated carrier counting technique as a function of hold-off time, at different V_{EX}, temperatures and gate frequencies, with T_{ON} = 2 ns. At 225 K and with f_{GATE} = 1 MHz, afterpulsing probability is just few percent, while it is almost 10 times higher with f_{GATE} = 10 MHz. At higher temperature (275 K), afterpulsing probability is strongly reduced because of faster release times for trapped carriers. Data are from a standard InGaAs/InP SPAD, but similar results have been achieved by a high-efficiency detector.

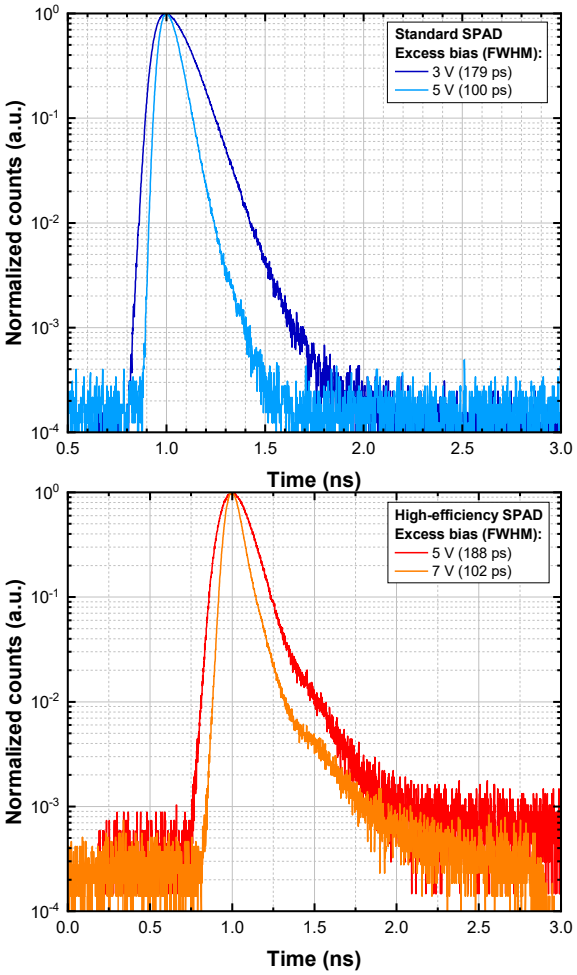

Figure 6 – Temporal response of standard (top) and high-efficiency SPAD (bottom) at different excess bias voltages V_{EX}, when illuminated by a 1550 nm pulsed laser (18 ps FWHM width).

Afterpulsing probability can be further reduced by employing the so-called "fast gating techniques", where the detector is rapidly turned ON and OFF at a frequency of more than 1 GHz, thus quenching any possible avalanche within few hundreds of picoseconds. Such very fast quenching guarantees very low afterpulsing probabilities, thus achieving photon count rates exceeding 500 Mcount/s [11].

We measured the timing response of our InGaAs/InP SPADs by focusing a 18 ps pulsed laser at 1550 nm in a 5 µm spot

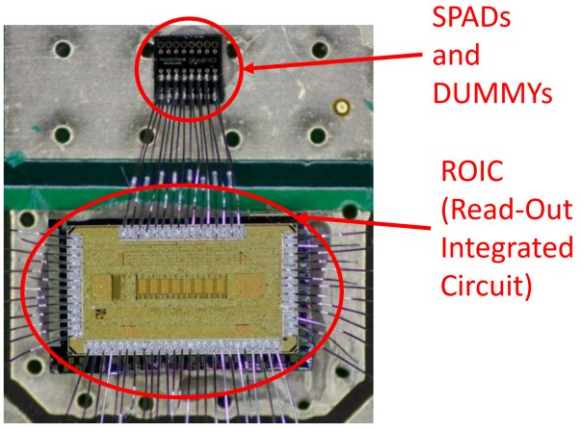

Figure 7 – Micrograph of a 8x1 SPAD array wire-bonded to a read-out integrated circuit.

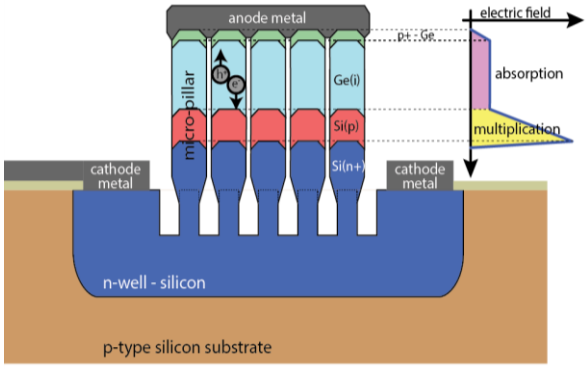

Figure 8 – Structure, doping and electric field profile of vertical Ge-on-Si SPADs. Vertical hetero-epitaxy allows to grown a germanium absorption layer on a silicon substrate.

inside the detector active area and employing a standard time-correlated single-photon counting technique. Figure 6 shows the temporal response of standard and high-efficiency SPADs at different V_{EX}: timing jitter is ~ 100 ps (FWHM) at respective typical operating conditions, i.e., V_{EX} = 5 V and V_{EX} = 7 V.

Next goal is the development of InGaAs/InP SPAD arrays. As a first step, we integrated a 8x1 InGaAs/InP SPAD array with a 8-channel read-out integrated circuit fabricated in 0.16 µm BCD technology (see a picture of the prototype under development in Figure 7). Its full experimental characterization is still in progress.

3. Ge-on-Si SPADs

The main drawbacks of InGaAs/InP SPADs are: i) maximum photon count rate is limited by afterpulsing effect; ii) they cannot be integrated with standard CMOS circuits. Ge-on-Si SPADs might overcome such limitations as they can be grown on silicon substrate and germanium-based SPAD already demonstrated lower afterpulsing compared to InGaAs/InP ones [12]. Germanium is employed for the absorption layer given its good absorption properties in the SWIR, despite its cut-off

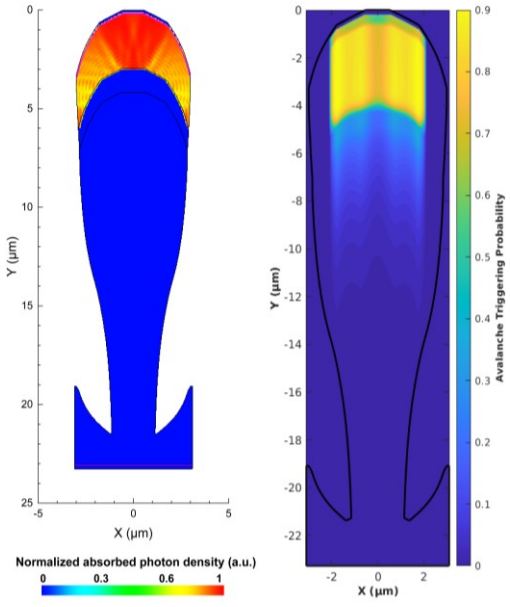

Figure 9 – FDTD optical simulation at 1550 nm (left) and avalanche triggering probability distribution (right) of the designed vertical Ge-on-Si SPAD.

reduction when deeply cooled, which lowers the detection efficiency at 1550 nm. However, many applications can properly work at shorter wavelength, in particular at 1310 nm.

Recent Ge-on-Si SPADs show a high DCR also at low temperature, because of the dislocations generated by conventional Ge/Si epitaxy [13]. As an alternative approach, we developed a novel technological platform, based on vertical hetero-epitaxy of Si and Ge micro-crystals, which enables the fabrication of SPADs and solid-state photomultipliers (SSPMs) with high photon detection efficiency and high fill-factor (see Figure 8). Thanks to the innovative vertical approach, the dislocations generating at Ge/Si interface are expelled towards the lateral surfaces of the micro-crystal, thus enabling the fabrication of low-DCR micro-crystal-based SPADs.

Figure 9 shows the optical and electrical design of a first device that will be soon fabricated. The absorption probability was estimated by means of finite-difference time-domain (FDTD) optical simulations, while avalanche triggering probability is calculated including the diffusion of minority carriers towards the high-field region. We estimated the PDE of the Ge-on-Si microSPAD (see Figure 10) and we expect more than 50% PDE at 1310 nm even with just 0.5 µm-thick Ge layer.

The fabrication and experimental characterization of such new vertical Ge-on-Si SPAD is currently in progress.

4. Conclusions

SWIR applications requiring practical (i.e., compact and cost-effective) single-photon detector currently rely on InGaAs/InP SPADs, which have good overall performance in terms of detection efficiency, dark count rate and timing jitter. However, their main limitations are the reduced maximum count rate and their non compatibility with CMOS read-out integrated circuits, which would ease their integration, the development of larger imagers and the cost reduction. To this aim, Ge-on-Si SPADs are currently under development, also exploiting new vertical growth approaches for tackling their main issue, i.e., the high defect concentration at the Ge/Si hetero-interface.

References

[1] F. Signorelli et al., “Low-Noise InGaAs/InP Single-Photon Avalanche Diodes for Fiber-Based and Free-Space Applications,” IEEE J. Sel. Top. Quantum Electron., vol. 28, no. 2, pp. 1–10, Mar. 2021.

[2] N. Gisin and R. Thew, “Quantum communication,” Nat. Photonics, vol. 1, no. 3, pp. 165–171, Mar. 2007.

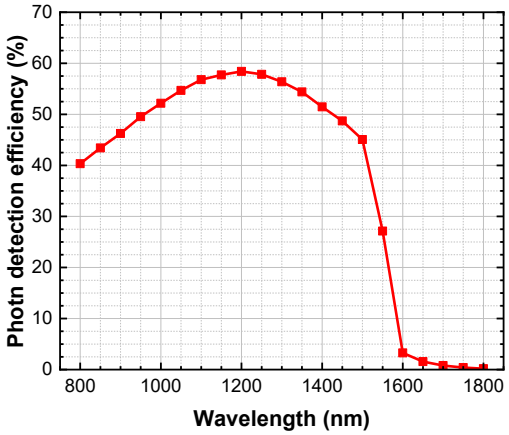

Figure 10 – Estimated photon detection efficiency at different wavelengths of the proposed Ge-on-Si SPAD.

[3] M. Davanço et al., “Telecommunications-band heralded single photons from a silicon nanophotonic chip,” Appl. Phys.

[4] Lett., vol. 100, no. 26, p. 261104, Jun. 2012.

[5] Y. U. Chao, M. Shangguan, X. I. A. Haiyun, J. Zhang, D. O. U. Xiankang, and J. W. Pan, “Fully integrated free-running InGaAs/InP single-photon detector for accurate lidar applications,” Opt. Express, vol. 25, no. 13, pp. 14611-14620, Jun. 2017.

[6] S. A. Carp et al., “Diffuse correlation spectroscopy measurements of blood flow using 1064 nm light,” J. Biomed. Opt., vol. 25, no. 09, pp. 97003–97004, Sep. 2020.

[7] L. F. Llin et al., “High sensitivity Ge-on-Si single-photon avalanche diode detectors,” Opt. Lett., vol. 45, no. 23, p. 6406, Dec. 2020.

[8] F. Acerbi, M. Anti, A. Tosi, and F. Zappa, “Design criteria for InGaAs/InP single-photon avalanche diode,” IEEE Photonics J., vol. 5, no. 2, pp. 6800209-6800209, April 2013.

[9] J. Ma et al., “Design considerations of high-performance InGaAs/InP single-photon avalanche diodes for quantum key distribution,” Appl. Opt., vol. 55, no. 27, p. 7497, Sep. 2016.

[10] F. Telesca, F. Signorelli, and A. Tosi, “Temperature-dependent photon detection efficiency model for InGaAs/InP SPADs,” Opt. Express, vol. 30, no. 3, pp. 4504–4514, 2022.

[11] C. Scarcella, G. Boso, A. Ruggeri, and A. Tosi, “InGaAs/InP single-photon detector gated at 1.3 GHz with 1.5 % afterpulsing,” IEEE J. Sel. Top. Quantum Electron., vol. 21, no. 3, pp. 17–22, 2015.

[12] P. Vines et al., “High performance planar germanium-on-silicon single-photon avalanche diode detectors,” Nat. Commun., vol. 10, no. 1, p. 1086, Dec. 2019.

[13] L. F. Llin et al., “High sensitivity Ge-on-Si single-photon avalanche diode detectors,” Opt. Lett., vol. 45, no. 23, p. 6406, 2020.